Two-Dimensional Heterospectral Correlation Analysis of X-ray Photoelectron Spectra and Infrared Spectra for Spin-Coated Films of Biodegradable Poly(3-hydroxybutyrate-*co*-3-hydroxyhexanoate) Copolymers

Hyun Chul Choi,[†] Soo Ryeon Ryu,[§] Ho Ji,[§] Seung Bin Kim,[∥] Isao Noda,[⊥] and Young Mee Jung*[,§]

Department of Chemistry, Chonnam National University, Gwangju 500-757, Korea, Department of Chemistry and Institute for Molecular Science and Fusion Technology, Kangwon National University, Chunchon 200-701, Korea, Department of Chemistry, POSTECH, Pohang 790-784, Korea, and The Procter & Gamble Company, West Chester, Ohio 45069

Received: April 13, 2010; Revised Manuscript Received: June 28, 2010

We investigated the thermal behavior of spin-coated films of biodegradable poly(3-hydroxybutyrate-*co*-3-hydroxyhexanoate) (P(HB-*co*-HHx)) copolymers at the molecular level. To better understand details of thermal behavior of spin-coated films of P(HB-*co*-HHx) copolymers, we applied two-dimensional (2D) correlation analysis to the spectra of P(HB-*co*-HHx) (HHx = 12.0, 10.0, and 3.8 mol %) copolymers during the heating process from 30 to 150 °C as obtained by temperature-dependent infrared-reflection absorption spectroscopy and X-ray photoelectron spectroscopy (XPS). 2D IR and 2D XPS correlation spectra of spin-coated films of P(HB-*co*-HHx) copolymers clearly revealed the sequence of intensity changes with increasing temperature: an amorphous band increases first and then a band for less ordered secondary crystals decreases before a band for well-ordered primary crystals. Furthermore, the synchronous 2D heterospectral XPS/IR correlation spectrum elucidated the correlation between the IR and XPS bands, confirming their band assignments. The asynchronous 2D heterospectral correlation spectrum revealed the probe-dependent asynchronicity between XPS and IR signals arising from the same species even under identical perturbation conditions because of the different scales of molecular changes probed. It clearly provides a complete interpretation of the phase transition phenomenon of P(HB-*co*-HHx) copolymers, which could not have been obtained through XPS or IR study alone, and also, the results obtained thereof offer a new insight into the molecular interactions as well observed by two different probes.

Introduction

Poly(hydroxyalkanoate) (PHA) polymers including poly(3-hydroxybutyrate) (PHB) and PHB-based copolymers, such as poly(3-hydroxybutyrate-*co*-3-hydroxyhexanoate) (P(HB-*co*-HHx)), are biodegradable and renewable polymers, which have been studied extensively as environment-friendly polymers.[1−4] The structure and thermal behavior of PHB and P(HB-*co*-HHx) copolymers have been investigated by X-ray diffraction, differential scanning calorimetry, FTIR spectroscopy, and two-dimensional (2D) correlation spectroscopy.[5−13] We have also recently investigated the transition temperature and thermal behavior of spin-coated films of P(HB-*co*-HHx) (HHx = 3.8, 7.2, and 10.0 mol %) copolymers by using principal component analysis-based 2D (PCA2D) correlation spectroscopy.[14,15]

X-ray photoelectrion spectroscopy (XPS) is known to provide valuable information about the local atomic environment of material surfaces.[16−18] By analyzing the photoelectron emitted following an incident X-ray beam, the binding energy can be determined. This energy is characteristic of each element, and can be slightly altered by the chemical state of the emitting atom. The peak areas can be used to determine the surface composition of constituent elements. Although XPS has many advantages, its application to the study of organic materials has been limited, partly because of the charging effect, which often complicates the data analysis.

Generalized 2D correlation spectroscopy is a well-established analytical technique that provides considerable utility and benefit in various spectroscopic studies of polymers.[19−21] Some of the notable features of generalized 2D correlation spectra are as follows: enhancement of spectral resolution by spreading peaks along the second dimension, establishment of unambiguous assignments through the correlation of bands selectively coupled by various interaction mechanisms, and determination of the sequence of the spectral peak emergence. A very intriguing method in 2D correlation spectroscopy is 2D heterospectral correlation analysis, where two completely different types of spectra for a system obtained by using multiple spectroscopic probes under a similar external perturbation are compared.[19,20,22−26] From the response patterns of the system monitored by two different probes under the same perturbation, one could detect a correlation between two spectral signals. For instance, 2D heterospectral correlation analysis between closely related spectroscopic measurements,[23,25] such as IR and Raman spectra, are very attractive from the point of better understanding its complementary vibration spectra. Such a combination provides especially rich insight and clarification into the in-depth study of vibrational spectra. Another type of the application of this technique is the heterocorrelation between completely different

* Author to whom correspondence should be addressed. Phone: +82-33-250-8495. Fax: +82-33-253-7582. E-mail: ymjung@kangwon.ac.kr.
[†] Chonnam National University.
[§] Kangwon National University.
[∥] POSTECH.
[⊥] The Procter & Gamble Company.

10.1021/jp103288x © 2010 American Chemical Society
Published on Web 07/26/2010

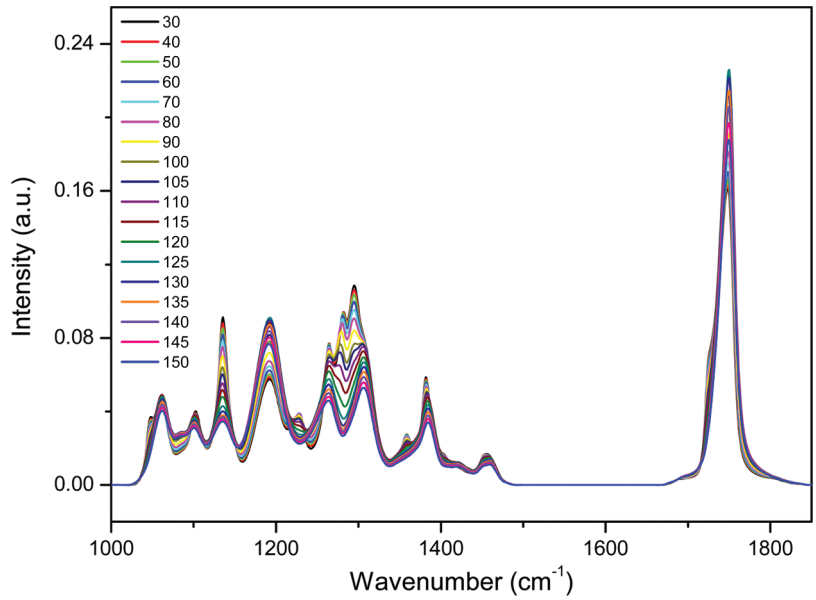

Figure 1. IRRAS spectra of a spin-coated film of P(HB-*co*-HHx) (HHx = 12.0 mol %) during heating from 30 to 150 °C at an interval of 5 °C.

types of spectroscopic or physical techniques, which is useful for investigating the structural and physical properties of materials under a particular external perturbation.[22,24,26] It has, for example, been applied to X-ray absorption and Raman spectroscopy.[24] Heterospectral correlation has become one of the most active areas of research in 2D correlation spectroscopy.

The objective of the present study is to better understand details of thermal behavior of spin-coated film of P(HB-*co*-HHx) copolymers at the molecular level. In this study, the thermal behavior of spin-coated films of P(HB-*co*-HHx) copolymers was characterized by FTIR and XPS. To obtain detailed information about the thermal behavior of P(HB-*co*-HHx) copolymers, we applied 2D correlation spectroscopy to the C1s XPS spectra and FTIR spectra during the heating process from 30 to 150 °C. We also undertook a 2D heterospectral XPS/IR correlation analysis, which has not yet been investigated for any polymers, to further explore the promising possibility of 2D correlation analysis to polymer material research.

Experimental Section

Biodegradable P(HB-*co*-HHx) (HHx = 12.0, 10.0, and 3.8 mol %) copolymers were obtained from the Procter & Gamble Company (Cincinnati, OH). It was dissolved in hot chloroform and then precipitated in hexane. The same process was repeated again, reprecipitated in methanol, and vacuum-dried at 60 °C. Pt-coated silicon wafers from Siltron Inc. (Korea) were used as the substrates for spin coating. To prepare spin-coated films, about 0.5 wt % P(HB-*co*-HHx) solutions dissolved in chloroform were spun onto a Pt-coated silicon wafer at 3500 rpm for 60 s. The thickness of the P(HB-*co*-HHx) spin-coated films was 60 nm. The spin-coated films were heated resistively at various temperatures up to 150 °C using a heating block. After heating, the films were annealed and cooled to room temperature for 10 min and then XPS spectra were measured.

The infrared-reflection absorption (IRRAS) spectra were measured at a spectral resolution of 4 cm^{-1} with a Bruker (Karlsruhe, Germany) IFS 66v/s FT-IR spectrometer equipped with a liquid-nitrogen-cooled MCT detector. A Bruker A513 reflection attachment, which includes a heating block attachment, was used for the IRRAS measurement, and a p-polarized infrared ray was used at an angle of incidence of 82°. The p-polarized infrared ray was generated by a SPECAC (Orpington, U.K.) wire-grid infrared polarizer. To ensure a high signal-to-noise ratio, 1024 interferograms were coadded for each measurement. Both sample and source compartment were evacuated to 1 mbar.

The XPS measurements were performed at the 8A1 beamline of the Pohang Accelerator Laboratory. X-rays were incident at an angle normal to the sample surface and the resulting photoelectrons were analyzed by an electron analyzer (Physical Electronics) located at an angle of 55° to the sample surface normal. The photon energy was 627 eV, and the energy resolving power ($E/\Delta E$) of the X-rays was better than 6000. The binding energy scale was calibrated by using the Au 4f feature at 83.96 ± 0.05 eV. The XPS peak was curve-fitted by Voigt profiles. Since the P(HB-*co*-HHx) copolymers are insulators, the binding energy determined from the XPS spectra is partially shifted because of the charging effect. This shift is of the order of several electronvolts, and varies with the X-ray intensity and the exposure time. Therefore, the contribution of the charging effect to the XPS spectrum must be removed to obtain the exact binding energy of the P(HB-*co*-HHx) copolymers. To remove the charging effect, the sample substrate was subjected to a bias voltage (10 V) during the XPS recording. We also carefully adjusted the photon flux, data acquisition time, and scan ranges.

Synchronous and asynchronous 2D correlation spectra were obtained using the same software as those described previously.[13−15,22−24] Prior to the 2D correlation calculations, normalization was applied to all of the measurements. In addition, baseline corrections and smoothing of all the measurements were performed before the 2D correlation calculations.

Results and Discussion

The temperature-dependent IRRAS spectra of a spin-coated film of P(HB-*co*-HHx) (HHx = 12.0 mol %) copolymer, obtained during the heating process from 30 to 150 °C, are shown in Figure 1. There are two distinct bands in the C═O stretching band, a crystalline band at 1726 cm^{-1} and an amorphous band near 1751 cm^{-1}. Figure 2a and b show the

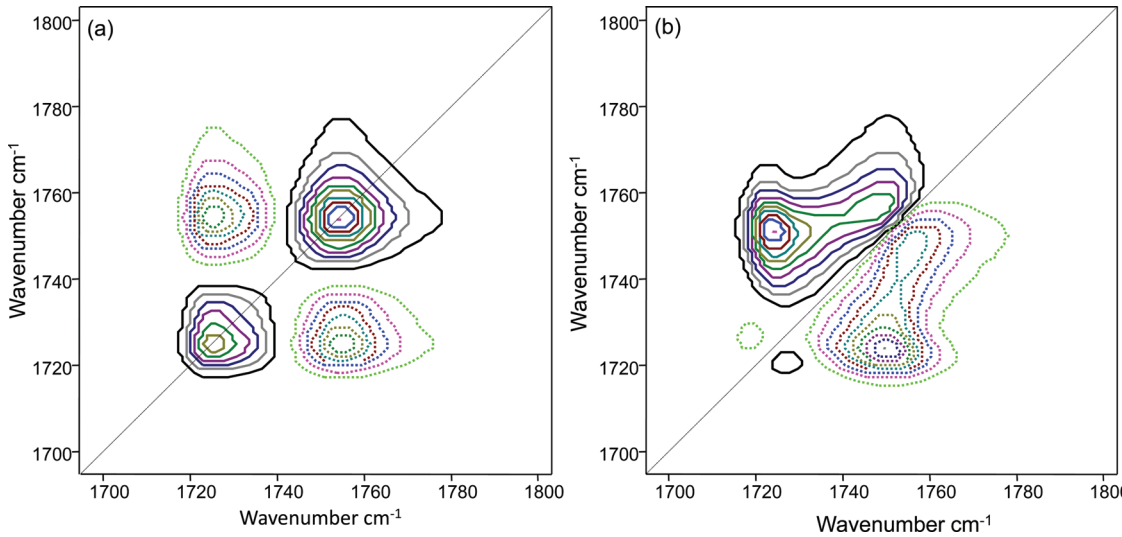

Figure 2. Synchronous (a) and asynchronous (b) 2D correlation spectra obtained from temperature-dependent IRRAS spectra of a spin-coated film of P(HB-*co*-HHx) (HHx = 12.0 mol %). The solid and dashed lines represent positive and negative cross peaks, respectively.

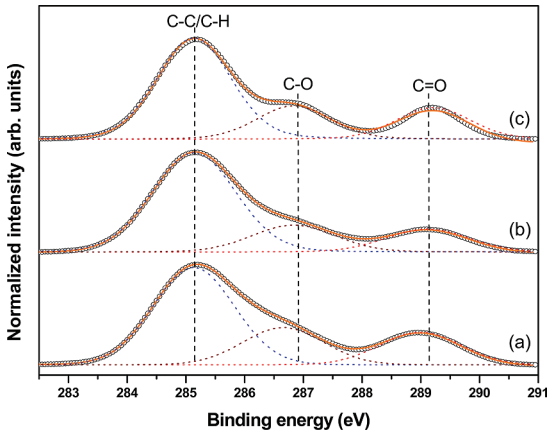

Figure 3. XPS C1s core-level spectra of a spin-coated film of P(HB-*co*-HHx) (HHx = 12.0 mol %) during the heating process: (a) 30 °C; (b) 110 °C; (c) 150 °C.

synchronous and asynchronous 2D correlation spectra in the C═O stretching bands constructed from the temperature-dependent IRRAS spectra of a spin-coated film of P(HB-*co*-HHx) copolymer during heating. In the synchronous 2D correlation spectrum, we can mainly observe the crystalline band at 1726 cm^{-1} and the amorphous band at 1751 cm^{-1}. However, the band at 1726 cm^{-1} now seems to be resolved into two bands at 1721 and 1730 cm^{-1} in the asynchronous 2D correlation spectrum, which is not readily detectable in the original 1D spectra. They correspond to the well-ordered primary crystals observed at a lower wavenumber and less ordered secondary crystals observed at a higher wavenumber. The analysis of 2D correlation spectra shows the following sequence of changes in spectral intensities with increasing temperature: 1751 → 1730 → 1721 cm^{-1}. It reveals that the intensity of an amorphous band is changing first and then that of a band for less ordered secondary crystals changes before that of a band for well-ordered secondary crystals with increasing temperature.

Figure 3 shows C1s core-level photoelectron spectra of a spin-coated film of P(HB-*co*-HHx) copolymer obtained during the heating process. Two bands can be resolved for all spectra. The asymmetric band centered at 285 eV is attributed to hydrocarbons (C—C or C—H).[27,28] A tail to the high binding energy suggests the presence of small amounts of ether carbons (C—O). The weak band at 289 eV is assigned to carbonyl carbon (C═O). Due to the similar spectral feature, however, it is difficult to obtain the detailed structural behavior of P(HB-*co*-HHx) copolymer from conventional 1D XPS spectra.

In order to investigate the details in the structural changes, we applied 2D correlation spectroscopy to the temperature-dependent XPS C1s core-level spectra of a spin-coated film of P(HB-*co*-HHx) (HHx = 12.0 mol %) copolymer. Figure 4 shows the synchronous and asynchronous 2D correlation spectra obtained from the temperature-dependent XPS C1s core-level spectra of a spin-coated film of P(HB-*co*-HHx) copolymer. As shown in Figure 4a, there are two bands near 289 eV assigned to C═O bond bands. Two bands at 288.3 and 289.3 eV, which are not readily noticeable in the 1D spectra of Figure 3, are clearly observed in the synchronous 2D correlation spectrum. The band at 288.3 eV can be assigned to carbonyl carbon in the crystalline structure, while the band at 289.3 eV is attributed to carbonyl carbon in the amorphous structure. Sato et al. examined the thermal behavior of the P(HB-*co*-HHx) copolymer using wide-angle X-ray diffraction (WAXD) measurements.[11] At room temperature, the P(HB-*co*-HHx) copolymer has an orthorhombic structure ($\alpha = \beta = \gamma = 90°$) with $a = 5.76$ Å, $b = 13.20$ Å, and $c = 5.96$ Å. The (110) d spacing of the P(HB-*co*-HHx) lattice is gradually increased with increasing temperature. This change corresponds to the decrease in the intermolecular force between the C═O group and the CH_3 group in the P(HB-*co*-HHx) copolymer. Since the XPS spectrum is obtained by the photoemitted electrons, the binding energy is very sensitive to the chemical environment of the element of interest. During the heating process, decreased intermolecular force enhances the bond strength around the carbonyl carbon in the P(HB-*co*-HHx) copolymer lattice, resulting in a high energy shift of the binding energy. In the present study, therefore, two bands at 288.3 and 289.3 eV can be assigned, respectively, to a crystalline carbonyl bond and an amorphous carbonyl bond.

The positive cross peaks at (284.3, 286.1), (284.3, 288.3), and (286.1, 288.3) eV show that the intensities of those bands decrease together during heating. However, the negative cross peaks at (284.3, 289.3), (286.1, 289.3), and (288.3, 289.3) eV show that the intensity of the band at 289.3 eV increases, while those at 284.3, 286.1, and 288.3 eV decrease. It reveals that a band at 289.3 eV is assignable to amorphous components, while the others are assigned to crystalline components. Particularly

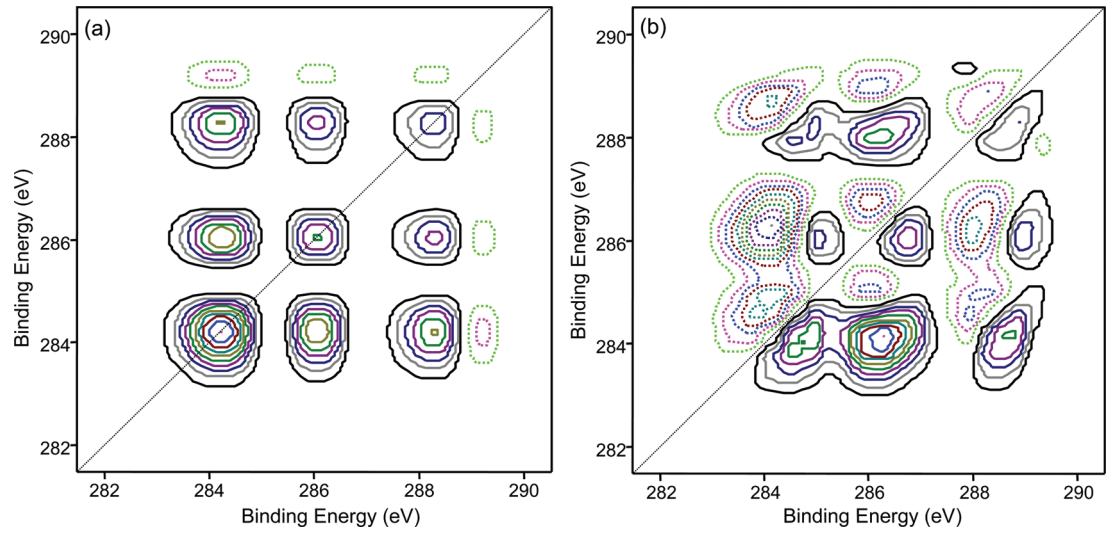

Figure 4. Synchronous (a) and asynchronous (b) 2D correlation spectra obtained from the temperature-dependent XPS C1s core-level spectra of a spin-coated film of P(HB-*co*-HHx) (HHx = 12.0 mol %). The solid and dashed lines represent positive and negative cross peaks, respectively.

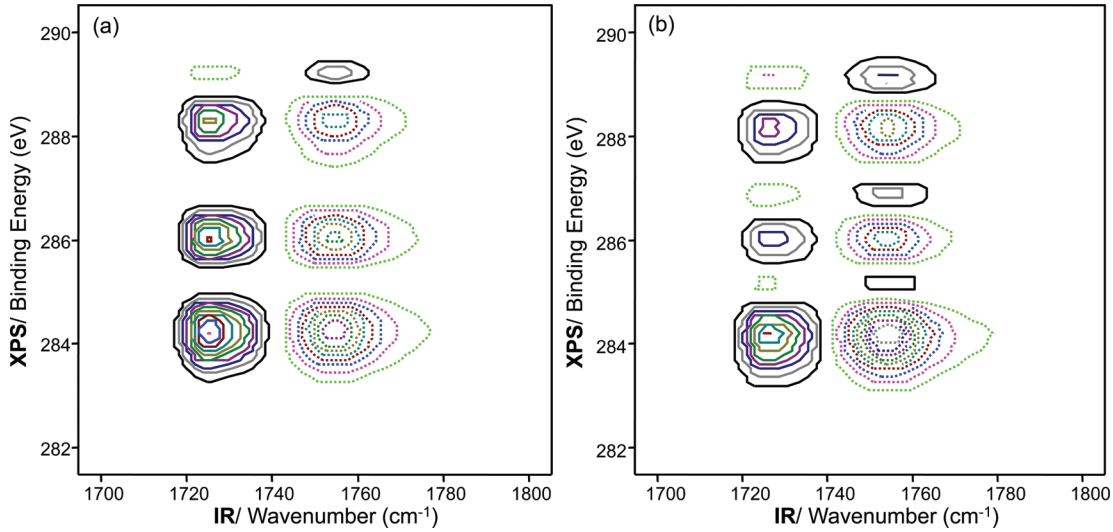

Figure 5. Synchronous (a) and asynchronous (b) heterospectral 2D XPS/IR correlation spectrum for a spin-coated film of P(HB-*co*-HHx) (HHx = 12.0 mol %). The solid and dashed lines represent positive and negative cross peaks, respectively.

interesting is that a band at 288.3 eV in the synchronous 2D correlation spectrum is clearly resolved into two bands at 288.8 and 287.9 eV in the asynchronous 2D correlation spectrum in Figure 4b. They correspond to the well-ordered primary crystals observed at a lower binding energy and less ordered secondary crystals observed at a higher binding energy in XPS spectra. From the sign of the cross peaks in the synchronous and asynchronous 2D correlation spectra, the intensity of a band at 289.3 eV changes first and then that at 288.8 eV changes before that at 287.9 eV. Most likely, the sequence of intensity changes with increasing temperature is such that the C═O band assigned to the amorphous component is changing first at an earlier (i.e., lower temperature) stage and then that for less ordered secondary crystals is changing before that for well-ordered secondary crystals at higher temperature. It is in good agreement with the analysis of 2D IR correlation spectra shown in Figure 2.

To ascertain the band assignment in the IR and XPS spectra of a spin-coated film of P(HB-*co*-HHx) copolymer, we performed a 2D heterospectral XPS/IR correlation analysis. Figure 5a shows the synchronous 2D heterospectral XPS/IR correlation spectrum. The positive cross peak in the synchronous 2D heterospectral correlation spectrum means that two bands sharing the cross peaks have the same origin, whereas a negative cross peak means that two bands sharing the cross peak have different origins. Thus, the positive cross peak at (1751 cm^{-1}, 289.3 eV) reveals that both the XPS band at 289.3 eV and the IR band at 1751 cm^{-1} are assigned to the C═O band for amorphous components. The negative cross peak at (1751 cm^{-1}, 288.3 eV) clearly shows that the XPS band at 288.3 eV and the IR band at 1751 cm^{-1} arise from different origins. Thus, the XPS band at 288.3 eV is assigned to the C═O band for crystalline components. It confirms again that bands at 288.3 and 289.3 eV are assignable, respectively, to crystalline and amorphous C═O bands. This conclusion is in good agreement with results from 2D IR and 2D XPS correlation spectra. Furthermore, the C—C or C—H XPS band at 284.3 eV and the C—O XPS band at 286.1 eV have negative cross peaks with the C═O IR band for amorphous components and negative cross peaks with that for crystalline components. This means that XPS bands to C—C (or C—H) and C—O arise from the crystalline components of P(HB-*co*-HHx) copolymer. The synchronous 2D heterospectral XPS/IR correlation spectrum clearly confirms that both the XPS band at 289.3 eV and the IR band at 1751 cm^{-1} are assigned to the C═O band for amorphous components.

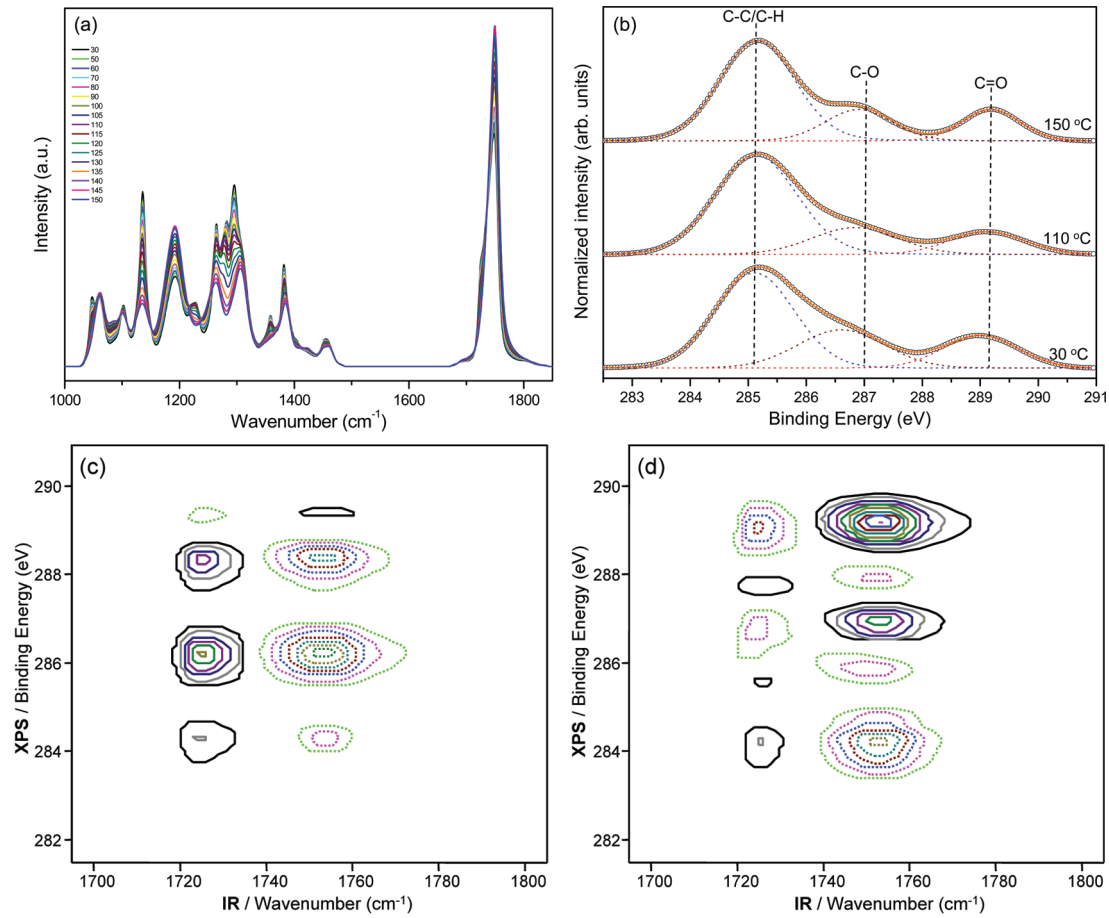

Figure 6. (a) IRRAS spectra of a spin-coated film of P(HB-*co*-HHx) (HHx = 10.0 mol %) during heating from 30 to 150 °C at an interval of 5 °C. (b) XPS C1s core-level spectra of a spin-coated film of P(HB-*co*-HHx) (HHx = 10.0 mol %) during the heating process. Synchronous (c) and asynchronous (d) heterospectral 2D XPS/IR correlation spectrum for a spin-coated film of P(HB-*co*-HHx) (HHx = 10.0 mol %). The solid and dashed lines represent positive and negative cross peaks, respectively.

The corresponding asynchronous 2D heterospectral XPS/IR correlation spectrum is shown in Figure 5b. From the cross peaks sign analysis, we can deduce the following sequence of events during the temperature increase: 1751 $cm^{-1} \rightarrow$ 1726 $cm^{-1} \rightarrow$ 289.3 eV $\rightarrow$ 288.3 eV. The sequential order of the intensity changes that intensity for amorphous components increases before those for crystalline components decrease are in good agreement with the separate result obtained by 2D IR and 2D XPS correlation studies. Interestingly, the 2D heterospectral correlation result also shows that the intensity changes of the IR bands occur before those of the XPS bands. It indicates that, even under identical perturbation conditions (temperature change in this study), some asynchronicity is observed between signals arising from the same species probed by two different techniques. This apparent probe-dependent asynchronicity is the result of the difference in the two analytical techniques (IR and X-ray) probing the slightly different aspects of molecular responses toward a given perturbation, like temperature change. In this study, spectral changes detected by the IR probe always occurred sooner (i.e., at a lower temperature) than those detected by XPS. Although XPS and IR spectra are both affected by rising temperature, the specific nature of the effect of temperature change on the IR spectrum is certainly very different from that of XPS. For example, features in the IR spectrum of a spin-coated film of P(HB-*co*-HHx) copolymer, which are directly related to the molecular vibrations of the system, are easily influenced by the temperature change, compared to the corresponding XPS spectrum. IR tends to be sensitive to longer range molecular interactions compared to more localized structures probed by X-rays. Thus, we can draw a much more detailed mechanistic picture of the phase transition process of this polymer system probed at different molecular scales. During the gradual melting of P(HB-*co*-HHx) copolymer by increasing temperature, the long-range order of the system appears to be disrupted first before localized structure changes. Thus, a seemingly simple phase transition phenomenon like melting of polymer crystals actually involves a different level of microscopic scales. Such insight could not have been obtained through XPS or IR study alone. Through 2D heterospectral correlation, one can unambiguously compare the subtle scale differences involved in the molecular interactions observed by two different probes.

To identify the mechanistic picture of the phase transition process of this polymer system, we performed the same analysis for spin-coated films of other P(HB-*co*-HHx) copolymers (HHx = 10.0 and 3.8 mol %). Figures 6 and 7 show the results of the same analysis of spin-coated films of other P(HB-*co*-HHx) copolymers, for HHx = 10 and 3.8 mol %, respectively. The results are exactly the same as our conclusion for a spin-coated film of P(HB-*co*-HHx) (HHx = 12.0 mol %). The fact that IR changes before XPS means the thermally induced phase transition like melting of polymer crystals starts with gradual disruption of the long-range order to the destruction of local order. There are multiple levels of molecular interaction scales involved in the process, which can be observed with different probes. IR may pick up the temperature-induced increase of the amorphous component earlier at a lower temperature than XPS. It clearly shows the surprising complexity of the even

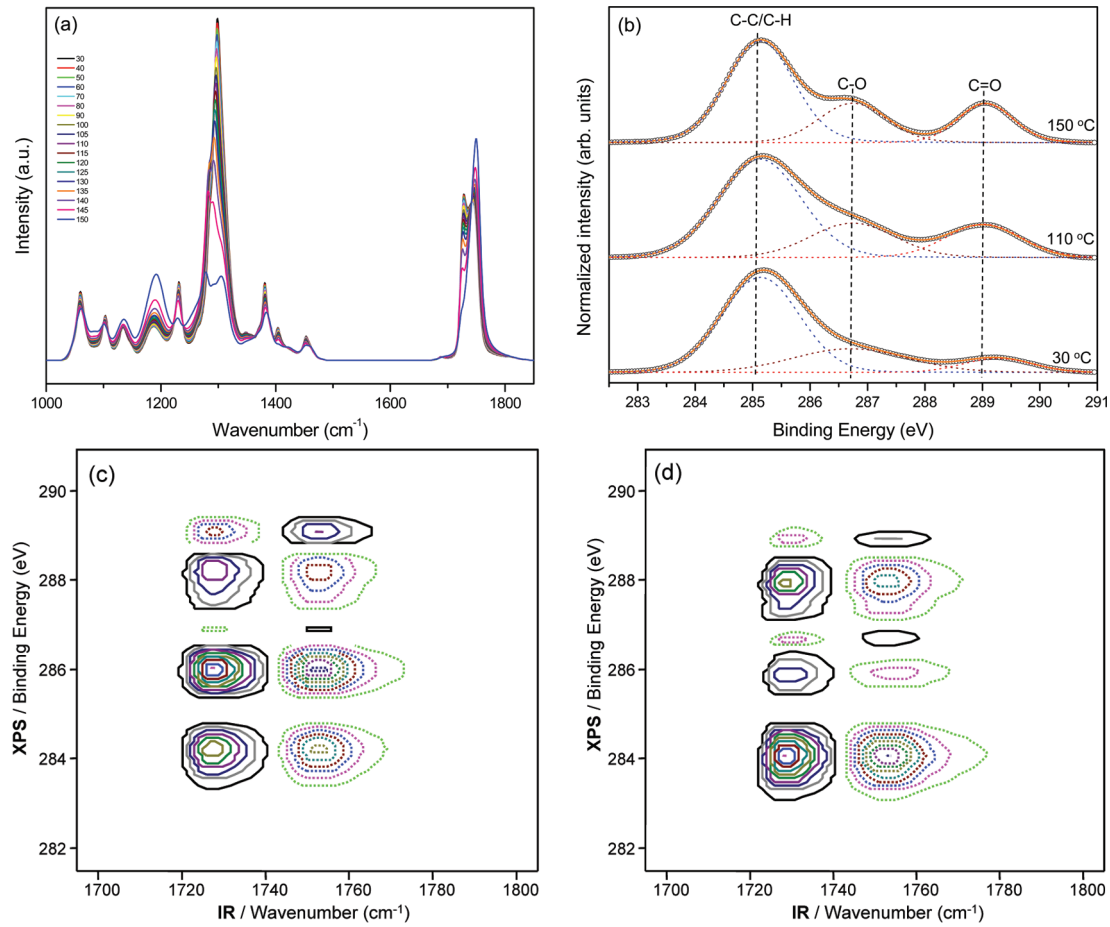

Figure 7. (a) IRRAS spectra of a spin-coated film of P(HB-*co*-HHx) (HHx = 3.8 mol %) during heating from 30 to 150 °C at an interval of 5 °C. (b) XPS C1s core-level spectra of a spin-coated film of P(HB-*co*-HHx) (HHx = 3.8 mol %) during the heating process. Synchronous (c) and asynchronous (d) heterospectral 2D XPS/IR correlation spectrum for a spin-coated film of P(HB-*co*-HHx) (HHx = 3.8 mol %). The solid and dashed lines represent positive and negative cross peaks, respectively.

seeming straightforward phase transition phenomenon, which could not have been obtained through XPS or IR study alone. This result gives very interesting insight into the unique feature of 2D heterospectral correlation analysis.

Conclusion

We have successfully demonstrated the thermal behavior of spin-coated films of biodegradable P(HB-*co*-HHx) (HHx = 12.0, 10.0, and 3.8 mol %) copolymers by using 2D IR, 2D XPS, and 2D heterospectral XPS/IR correlation analyses. 2D IR correlation spectra show the sequence of intensity changes with increasing temperature is such that an amorphous band is increasing first and then a band for less ordered secondary crystals decreases before a band for well-ordered primary crystals.

2D XPS correlation spectra show that there are two bands near 289.0 eV assigned to C═O bond bands. Two bands at 288.3 and 289.3 eV, which are not readily noticeable in the 1D spectra, are clearly observed in the synchronous 2D correlation spectrum. The C═O band at 288.3 eV is assigned to the crystalline structure, while the band at 289.3 eV is attributed to the amorphous structure. The crystalline C═O band at 289.3 eV in the synchronous 2D spectrum is clearly resolved into two bands at 288.8 and 287.9 eV in the asynchronous 2D correlation spectrum. The two bands correspond to the well-ordered primary crystals observed at a lower binding energy and less ordered secondary crystals observed at a higher binding energy. Thus, 2D correlation analysis gives much greater spectral resolution than the peak fitting method which is usually used in spectral analysis.

Furthermore, the synchronous 2D heterospectral XPS/IR correlation spectrum clearly demonstrates that an XPS band at 289.3 eV and a band near 288.3 eV are, respectively, assigned to amorphous and crystalline components. The asynchronous 2D heterospectral XPS/IR correlation spectrum shows a very interesting sequential order of the intensity changes that spectral changes detected by the IR probe always occurred sooner (i.e., at a lower temperature) than those detected by XPS. It shows that the phase transition of P(HB-*co*-HHx) copolymer by increasing temperature actually involves a different level of microscopic scales. During the gradual melting process, the long-range molecular interactions detected by the IR probe appear first before more localized structure changes detected by XPS. This observed probe-dependent asynchronicity must therefore reflect the subtle difference in the selectivity and specificity of these probes toward molecular scale changes induced by the applied perturbation. The 2D heterospectral XPS/IR correlation analysis has confirmed some band assignments and has provided new insight into the correlation between XPS and IR bands, which had not been possible from a simple examination of XPS or IR spectra alone.

Acknowledgment. This work was supported by the National Research Foundation of Korea (NRF) grants funded by the Korea government (MEST) (Nos. 2009-0065428 and 2009-

0087013) and the BK 21 program from the Ministry of Education, Science and Technology of Korea. This study was financially supported by Chonnam National University, 2007. The authors thank Pohang Accelerator Laboratory (PAL) for XPS measurement.

References and Notes

(1) Bastiolo, C. In *Handbook of Biodegradable Polymers*; Rapra Technology Limited: U.K., 2005.

(2) Chiellini, E.; Solaro, R. In *Recent Advances in Biodegradable Polymers and Plastics*; Wiley-VCH: Weinheim, Germany, 2003.

(3) Satkowski, M. M.; Melik, D. H.; Autran, J.-P.; Green, P. R.; Noda, I.; Schechtman, L. A. In *Biopolymers*; Steinbüchel, A., Doi, Y., Eds.; Wiley-VCH: Weinheim, Germany, 2001; p 231.

(4) Noda, I.; Green, P. R.; Satkowski, M. M.; Schechtman, L. A. *Biomacromolecules* **2000**, *6*, 580.

(5) Sato, H.; Mori, K.; Murakami, R.; Ando, Y.; Takahashi, I.; Zhang, J.; Terauchi, H.; Hirose, F.; Senda, K.; Tashiro, K.; Noda, I.; Ozaki, Y. *Macromolecules* **2006**, *39*, 1525.

(6) Sato, H.; Murakami, R.; Zhang, J.; Mori, K.; Takahashi, I.; Terauchi, H.; Noda, I.; Ozaki, Y. *Macromol. Symp.* **2005**, *230*, 158.

(7) Sato, H.; Murakami, R.; Padermshoke, A.; Hirose, F.; Senda, K.; Noda, I.; Ozaki, Y. *Macromolecules* **2004**, *37*, 7203.

(8) Sato, H.; Murakami, R.; Padermshoke, A.; Yamaguchi, H.; Terauchi, H.; Ekgasit, S.; Noda, I.; Ozaki, Y. *Macromolecules* **2004**, *37*, 3763.

(9) Furukawa, T.; Sato, H.; Murakami, R.; Zhang, J.; Duan, Y.-X.; Noda, I.; Ochiai, S.; Ozaki, Y. *Macromolecules* **2005**, *38*, 6445.

(10) Zhang, J.; Sato, H.; Furukawa, T.; Tsuji, H.; Noda, I.; Ozaki, Y. *J. Phys. Chem. B* **2006**, *110*, 24463.

(11) Zhang, J.; Duan, Y.; Sato, H.; H.; Noda, I.; Yan, S.; Ozaki, Y. *Macromolecules* **2005**, *38*, 8012.

(12) Zhang, J.; Sato, H.; Noda, I.; Ozaki, Y. *Macromolecules* **2005**, *38*, 4274.

(13) Jung, Y. M.; Sato, H.; Noda, I. *Anal. Sci.* **2007**, *23*, 881.

(14) Ji, H.; Kim, S. B.; Noda, I.; Jung, Y. M. *Spectrochim. Acta, Part A* **2009**, *71*, 1873.

(15) Ji, H.; Hwang, H.; Kim, S. B.; Noda, I.; Jung, Y. M. *J. Mol. Struct.* **2008**, *883*−*884*, 167.

(16) Hufner, S. *Photoelectron Spectroscopy*, 2nd ed.; Springer: Heidelberg, Germany, 1996.

(17) Ghosh, P. K. *Introduction to Photoelectron Spectroscopy*; John Wiley & Sons, Inc.: New York, 1983.

(18) Jablonski, A. *Surf. Sci.* **2009**, *603*, 1342.

(19) Noda, I.; Ozaki, Y. *Two-Dimensional Correlation Spectroscopy: Applications in Vibrational Spectroscopy*; John Wiley & Sons, Inc.: New York, 2004.

(20) Jung, Y. M.; Noda, I. *Appl. Spectrosc. Rev.* **2006**, *41*, 515.

(21) Noda, I. *Appl. Spectrosc.* **1993**, *47*, 1329.

(22) Kim, H. J.; Kim, S. B.; Kim, J. K.; Jung, Y. M. *J. Phys. Chem. B* **2006**, *110*, 23123.

(23) Schultz, G.; Jirasek, A.; Blades, M. W.; Turner, R. F. B. *Appl. Spectrosc.* **2003**, *57*, 156.

(24) Choi, H. C.; Jung, Y. M.; Noda, I.; Kim, S. B. *J. Phys. Chem. B* **2003**, *107*, 5806.

(25) Jung, Y. M.; Czarnik-Matusewicz, B.; Ozaki, Y. *J. Phys. Chem. B* **2000**, *104*, 7812.

(26) Noda, I. *Chemtracts: Macromol. Chem.* **1990**, *1*, 89.

(27) Zheng, Z.; Bei, F.-F.; Tian, H.-L.; Chen, G.-Q. *Biomaterials* **2005**, *25*, 3537.

(28) Qu, X.-H.; Wu, Q.; Liang, J.; Qu, X.; Wang, S.-G.; Chen, G.-Q. *Biomaterials* **2005**, *26*, 6991.

JP103288X